AIP | The Journal of Chemical Physics

Spin-orbit coupling calculations with the two-component normalized elimination of the small component method

Michael Filatov, Wenli Zou, and Dieter Cremer

Citation: J. Chem. Phys. **139**, 014106 (2013); doi: 10.1063/1.4811776
View online: http://dx.doi.org/10.1063/1.4811776
View Table of Contents: http://jcp.aip.org/resource/1/JCPSA6/v139/i1
Published by the AIP Publishing LLC.

Spin-orbit coupling calculations with the two-component normalized elimination of the small component method

Michael Filatov, Wenli Zou, and Dieter Cremer
Department of Chemistry, Southern Methodist University, 3215 Daniel Ave., Dallas, Texas 75275-0314, USA

(Received 10 March 2013; accepted 9 June 2013; published online 2 July 2013)

A new algorithm for the two-component Normalized Elimination of the Small Component (2cNESC) method is presented and tested in the calculation of spin-orbit (SO) splittings for a series of heavy atoms and their molecules. The 2cNESC is a Dirac-exact method that employs the exact two-component one-electron Hamiltonian and thus leads to exact Dirac SO splittings for one-electron atoms. For many-electron atoms and molecules, the effect of the two-electron SO interaction is modeled by a screened nucleus potential using effective nuclear charges as proposed by Boettger [Phys. Rev. B **62**, 7809 (2000)]. The use of the screened nucleus potential for the two-electron SO interaction leads to accurate spinor energy splittings, for which the deviations from the accurate Dirac Fock-Coulomb values are on the average far below the deviations observed for other effective one-electron SO operators. For hydrogen halides HX (X = F, Cl, Br, I, At, and Uus) and mercury dihalides HgX_2 (X = F, Cl, Br, I) trends in spinor energies and SO splittings as obtained with the 2cNESC method are analyzed and discussed on the basis of coupling schemes and the electronegativity of X.
 [http://dx.doi.org/10.1063/1.4811776]

I. INTRODUCTION

The normalized elimination of the small component (NESC) method, originally developed by Dyall[1,2] is a first principles 2-component approach where the electron and the positron states are decoupled via elimination of the small component of the relativistic wavefunction. NESC is regarded as a *Dirac-exact* relativistic method in view of the fact that, for one-electron atoms, it is fully equivalent to the 4-component Dirac equation.[3] In a series of previous publications, we developed and implemented a new algorithm for NESC,[4] which makes it possible to routinely carry out scalar-relativistic calculations for large molecules with heavy atoms. In addition, we worked out the methodology for calculating first order response properties,[5] such as the atomic forces needed for the calculation of the equilibrium geometry of a molecule, the electric dipole moment of a molecule,[6] EPR hyperfine structure constants,[7] contact densities for the calculation of Mössbauer isomer shifts,[8] or electric field gradients for nuclear quadrupole coupling constants.[9] In follow-up work, we developed the methodology for NESC second order response properties,[10] which is needed for the analytic calculation of vibrational frequencies,[6,10] static electric polarizabilities, or infrared intensities.[6] We demonstrated the usefulness of the NESC method when calculating free energy differences of organic tweezers complexes with different metal ions, especially mercury ions,[11] or determining the size of the gold nucleus in different isotopomers with the help of its quadrupole anomaly.[12] In this work, we will extend our previous scalar relativistic investigations to include the spin-orbit interaction into the NESC method in a form that allows this method to be used for the calculation of large molecular systems and for obtaining their first and second order response properties via the analytic derivatives formalism.

Spin-orbit coupling (SOC) is a relativistic effect,[13–20] which results in the splitting of the orbital energy levels (especially the *p*-levels of heavy atoms) according to the *jj*-coupling scheme, changes molecular spectra by making spin symmetry-forbidden transitions possible, has an impact on molecular reactions by enabling intersystem crossings, and is relevant for the calculation of dissociation energies and reaction energies in general when heavy atoms with atomic number $Z > 36$ are involved.[21] The calculation of SOC with NESC requires a two-component formulation (2cNESC) as it was originally developed by Dyall.[1,13]

Typically, the SOC operator is split into a one- and a two-electron part. At the lowest level of relativistic approximation, both parts are contained in the Breit-Pauli operator, which has been implemented by Werner and co-workers for its use with correlated wavefunctions[22] (see also Ref. 23). For heavy elements, SOC is dominated by the one-electron terms. The two-electron SO terms often reduce the former terms by about 5% for elements with a filled 5d shell and by about 10% in the case of elements with a filled 6d shell (see below), which is an indication of their overall screening effect. These contributions are not negligible; however, in most cases they vary parallel with the one-electron SO terms.[24] There are only a few cases known where the two-electron contributions take unusual values and a genuine SOC operator with explicit one and two-electron part is required.[25,26]

In view of the much smaller two-electron contributions and the significantly larger costs to calculate them,[27] several simplification schemes have been suggested, which aim to estimate the magnitude of the two-electron part once the one-electron SO part has been calculated accurately, i.e., SOC is calculated with an *effective one-electron SOC operator*. To be mentioned in this connection are the

mean-field SOC operator of Hess *et al.*,[28] the related atomic mean field integral (AMFI) approach, which was developed in form of an efficient computer code by Schimmelpfennig,[29] or the screened-nuclear-spin-orbit (SNSO) approach of Boettger,[30] in which the two-electron contributions to SOC are considered by appropriate screening of the nuclear potential, i.e., the use of effective nuclear charges. The SNSO approach was formulated within the Douglas-Kroll-Hess quasirelativistic approximation of relativistic effects[31–33] and since it presented a significant simplification of the calculation of SOC effects, it was adopted by several authors in the following years in the same or a slightly modified way.[34–36]

The 2cNESC method presented here includes the effective one-electron SOC operator of Boettger and is based on the general Hartree-Fock (GHF) formalism[37,38] for many-electron systems. We will speak of a 2cNESC method when one-electron systems have to be calculated and a 2cNESC(SNSO) method when many-electron systems are described. In this connection, we mention that methods closely related to NESC have been developed and terms such as XQR (exact quasi-relativistic), IOTC (infinite order two-component),[39] or X2C (exact two-component) have been coined. The recent review article by Peng and Reiher[19] defines these terms. There seems to be a tendency to exclusively use the term X2C in the sense of an *one-step exact decoupling transformation 2-component approach* provided certain requirements are fulfilled. Unfortunately, other authors used X2C in connection with spin-free Dirac-exact methods, which leads to some confusion. To avoid any confusion, we use the term Dirac-exact 2-component NESC (2cNESC) for the method described in this work.

With the 2cNESC method, we will investigate SO splittings in a series of atoms and molecules. In Sec. II, we present the basic theory for 2cNESC(SNSO)/GHF. In Sec. III, computational details of our SOC investigation are described and in Sec. IV, results for a series of atoms and molecules are analyzed and discussed. Finally, Sec. V summarizes the conclusions of our SOC investigation.

II. DETAILS OF A TWO-COMPONENT NESC METHOD

The NESC method[1,4] provides the exact electronic solutions of the full 4-component Dirac equation by solving a set of coupled 2-component equations. Starting from the modified Dirac equation[1,13] (1) in matrix form,

$$\begin{pmatrix} \mathbf{V} & \mathbf{T} \\ \mathbf{T} & \mathbf{W}-\mathbf{T} \end{pmatrix} \begin{pmatrix} \mathbf{A}_- & \mathbf{A}_+ \\ \mathbf{B}_- & \mathbf{B}_+ \end{pmatrix} = \begin{pmatrix} \mathbf{S} & \mathbf{0} \\ \mathbf{0} & (2mc^2)^{-1}\mathbf{T} \end{pmatrix} \begin{pmatrix} \mathbf{A}_- & \mathbf{A}_+ \\ \mathbf{B}_- & \mathbf{B}_+ \end{pmatrix} \begin{pmatrix} \mathbf{E}_- & \mathbf{0} \\ \mathbf{0} & \mathbf{E}_+ \end{pmatrix}, \quad (1)$$

where **S**, **T**, and **V** represent the overlap, the kinetic, and the potential energy matrices, **W** is the matrix of the operator $(\boldsymbol{\sigma}\cdot\mathbf{p})V(\mathbf{r})(\boldsymbol{\sigma}\cdot\mathbf{p})/4m^2c^2$, and the $\mathbf{A}_\pm$ and $\mathbf{B}_\pm$ are the large and the pseudo-large components of the electronic (+ subscript) and positronic (− subscript) states with energies E_+ and E_-, respectively, Dyall[1] has derived a set of Eqs. (2),

$$\tilde{\mathbf{L}}\mathbf{A}_+ = \tilde{\mathbf{S}}\mathbf{A}_+\mathbf{E}_+, \quad (2a)$$

$$\tilde{\mathbf{L}} = \mathbf{U}^\dagger\mathbf{T} + \mathbf{T}\mathbf{U} - \mathbf{U}^\dagger(\mathbf{T}-\mathbf{W})\mathbf{U} + \mathbf{V}, \quad (2b)$$

$$\tilde{\mathbf{S}} = \mathbf{S} + \frac{1}{2mc^2}\mathbf{U}^\dagger\mathbf{T}\mathbf{U}, \quad (2c)$$

where the NESC one-electron Hamiltonian $\tilde{\mathbf{L}}$ and the relativistic wavefunction metric $\tilde{\mathbf{S}}$ are defined using the elimination of the small component (ESC) operator $\hat{U}$, which connects the large and the pseudo-large components of the relativistic electronic wavefunction via Eq. (3):

$$\mathbf{B}_+ = \mathbf{U}\mathbf{A}_+. \quad (3)$$

The ESC matrix **U** can be obtained by iterating Eq. (4),

$$\mathbf{U} = \mathbf{T}^{-1}\left(\mathbf{S}\tilde{\mathbf{S}}^{-1}\tilde{\mathbf{L}} - \mathbf{V}\right), \quad (4)$$

together with Eqs. (2b) and (2c).[2,4] Alternatively, the ESC matrix can be deduced from the electronic solutions of the modified Dirac equation (1) by using Eq. (5),[1,4]

$$\mathbf{U} = \mathbf{B}\mathbf{A}^{-1} = \mathbf{B}\mathbf{A}^\dagger\left(\mathbf{A}\mathbf{A}^\dagger\right)^{-1}. \quad (5)$$

The one-step method of solving the NESC equations was originally proposed by Dyall[1] and later used by Zou *et al.*[4] in practical calculations using NESC.

The NESC method is typically employed in its spin-free (sf) form, which is achieved by separating the sf and spin-dependent parts of the **W** matrix as in Eq. (6),

$$\mathbf{W} = \mathbf{W}^{sf} + i\boldsymbol{\sigma}\cdot\mathbf{W}^{SO}. \quad (6)$$

The separation is achieved by the use of the Dirac identity $(\boldsymbol{\sigma}\cdot\mathbf{A})(\boldsymbol{\sigma}\cdot\mathbf{B}) = \mathbf{A}\cdot\mathbf{B} + i\boldsymbol{\sigma}\cdot\mathbf{A}\times\mathbf{B}$ and the spin-free and the spin-orbit (SO) parts of the **W** matrix are defined as in Eq. (7):

$$\mathbf{W}^{sf}_{\bar{\mu}\bar{\nu}} = -\langle\bar{\mu}|\frac{1}{4m^2c^2}\nabla\times V(\mathbf{r})\nabla|\bar{\nu}\rangle, \quad (7a)$$

$$\mathbf{W}^{SO}_{\bar{\mu}\bar{\nu}} = -\langle\bar{\mu}|\frac{1}{4m^2c^2}\nabla\times V(\mathbf{r})\nabla|\bar{\nu}\rangle. \quad (7b)$$

In these equations, a spinor basis set $\bar{\chi}$ is used which comprises basis functions for both directions of spin, α and β. The sf-NESC formalism is obtained by neglecting the SO part of the **W** matrix.[4] In the sf-formalism, a spin-independent basis set χ can be used, which results in reducing the dimension of all the matrices in Eqs. (1) and (2) by a factor of two. Although it may seem impractical to solve Eqs. (1) and (2) in the spin-dependent form, these equations should be solved for one-electron potential (e.g., electron-nuclear attraction potential) only, which, even for a very large system comprising several thousands of basis functions, takes only a fraction of the time required to solve the self-consistent field equations.[4]

The one-electron NESC Hamiltonian $\tilde{\mathbf{L}}$ obtained by solving Eqs. (1), (2), and (5) or Eq. (4) has to be renormalized for multi-electron systems according to[13,40]

$$\mathbf{H}^{NESC}_{1e} = \mathbf{G}^\dagger\tilde{\mathbf{L}}\mathbf{G}. \quad (8)$$

A renormalization matrix that possesses the correct transformation properties and avoids the so-called *picture change error* is given in Eq. (9),[41]

$$\mathbf{G} = \mathbf{S}^{-1/2}\left(\mathbf{S}^{1/2}\tilde{\mathbf{S}}^{-1}\mathbf{S}^{1/2}\right)^{1/2}\mathbf{S}^{1/2}. \quad (9)$$

In the sf case, the use of the renormalized one-electron Hamiltonian $\mathbf{H}_{1e}^{NESC}$ in connection with the non-relativistic many-electron formalism represents a very accurate approximation to the exact Foldy-Wouthuysen formalism as it neglects only a tiny fraction of the relativistic two-electron terms.[13,40]

When the SO terms are taken into the account, the use of the bare nuclear potential in Eq. (7b) typically leads to a serious overestimation of the SO splittings in many-electron atoms and molecules. The effect of missing two-electron SO contributions can be sufficiently accurately modeled by the SNSO approximation of Boettger.[30] (For recent work with the SNSO approach, see Peng and Reiher.[19]) Within this approximation, the SO terms of the one-electron NESC Hamiltonian are scaled by using basis-function-dependent scaling factors to simulate the effect of the missing two-electron SO terms:

$$\left(\mathbf{H}_{1e,SNSO}^{NESC}\right)_{\bar{\mu}\bar{\nu}} = \left(\mathbf{H}_{1e,SO}^{NESC}\right)_{\bar{\mu}\bar{\nu}} - \sqrt{\frac{Q(l_{\bar{\mu}})}{Z_{\bar{\mu}}}}\left(\mathbf{H}_{1e,SO}^{NESC}\right)_{\bar{\mu}\bar{\nu}}\sqrt{\frac{Q(l_{\bar{\nu}})}{Z_{\bar{\nu}}}}. \quad (10)$$

In Eq. (10), $Z_{\bar{\mu}}$ is the charge of the nucleus at which the spinor basis function $\bar{\mu}$ is centered and $Q(l_{\bar{\mu}})$ is a screening factor that depends on the orbital angular momentum of the function $\bar{\mu}$, $Q(l) = 0, 2, 10, 28, \cdots$ for $l = 0, 1, 2, 3, \cdots$. For the virtual spinors with $Q(l_{\bar{\mu}}) \geq Z_{\bar{\mu}}$, this SNSO often leads to qualitatively incorrect SO splittings resulting from the fact that the number of screened electrons is overestimated. Based on comparisons with the 4cDirac/HF SO splittings, we suggest a modified $Q'(l)$ parameter calculated by

$$Q'(l) = \begin{cases} Q(l) & (Z > Q(l)) \\ Q(l') & (Z \leq Q(l)) \end{cases}, \quad (11)$$

where l' is the maximum l value which makes $Z > Q(l')$. Calculations on atoms with Z ranging from 1 to 120 with $l \leq 6$ (i-type basis functions) show that this modification leads to an agreement of the SO splittings within 0.02 hartree, for spinors with $j \geq 7/2$.

The accuracy of the original SNSO method can be improved by using slightly adjusted parameters for the p-, d-, and f-type basis functions. Using $Q(d) = 11.0$, $Q(f) = 28.84$, and $Q(p) = 2.34\,Erf(34500/\alpha_p)$, where α_p is the Gaussian exponential parameter of the p-type basis function, the relative deviation of the calculated SO splittings from the reference 4cDirac/HF values is reduced by a factor of two. The original SNSO screening factors imply that, for electrons in p-type orbitals, the nuclear charge is completely screened by the deepest core 1s electrons. The proposed dependence of the $Q(p)$ screening factor on the exponential parameter of the basis function makes it possible to model penetration of these electrons into the K-shell and, just with the use of a one-parameter function (the error function), to improve the SO splittings for p-spinors considerably. The parameters for the new screening factors were obtained by fitting the calculated SO splittings to the reference 4cDirac/HF values for noble gas atoms Xe and Rn. In the following, the results obtained using the modified SNSO scheme will be labeled 2cNESC(mSNSO).

We tested also another approximate SO calculation based on a suggestion by Li *et al.*[42] who approximated the two-component relativistic one-electron Hamiltonian by

$$\mathbf{H}^{high} \approx \mathbf{H}_{sf}^{high} + \left(\mathbf{H}^{low} - \mathbf{H}_{sf}^{low}\right), \quad (12)$$

where a *high* level method is used for the scalar relativistic part (*sf* denotes *spin-free*) and a *low* level approach for the SO calculations. We used in this connection NESC and IORA (Infinite Order Regular Approximation);[43,44] however, results obtained in this way were inferior to those obtained with 2cNESC(mSNSO) and therefore we will discuss here only the latter.

The renormalized 2cNESC(SNSO) or 2cNESC(mSNSO) effective one-electron operator obtained by the procedure described above can be conveniently used in connection with the GHF or general Kohn-Sham (GKS) formalism for obtaining the total energy and spinor energies of many-electron systems.[37,38,45] In Secs. III and IV, the accuracy of the 2cNESC(SNSO) and 2cNESC(mSNSO) procedures will be investigated by the calculation of a representative set of atoms and molecules.

III. COMPUTATIONAL TECHNIQUES

The algorithms described above have been programmed within the COLOGNE2012 program package.[46] This implied the inclusion of the GHF routine, the programming of the **W**-integrals, and the set up of the 2cNESC algorithm. The 2cNESC and 2cNESC(SNSO) calculations were carried out with a variety of uncontracted basis sets (compare with Table I). The calculations of the atoms were carried out with an uncontracted 32s30p20d15f basis where the exponents were generated by the formula[47,48]

$$\exp(-3.84 + 0.72 \times (i-1)), \quad i = 1, 2, \ldots, N_l \quad (13)$$

with $N_l = 32$ for s-, 30 for p-, 20 for d-, and 15 for f-type functions. For reference calculations of the 4cDirac/HF-type, the relativistic program DIRAC was used.[49]

2cNESC(SNSO) calculations of molecules HX and HgX_2 were performed with the uncontracted cc-pVTZ basis set of Dunning[50,51] in the case of $Z < 18$ and Dyall's uncontracted TZ basis set augmented with diffuse and polarization functions[52–55] for heavier atoms. The bond lengths of HX molecules were chosen to be either the experimental (where available) or reliable quantum chemical r_e values: 0.917 (HF[56]), 1.275 (HCl[56]), 1.414 (HBr[56]), 1.609 (HI[56]), 1.738 (HAt[57]), and 1.949 Å(HUus[58]), respectively. The bond lengths of the HgX_2 molecules were taken from Kim *et al.*:

TABLE I. Uncontracted basis functions used in the molecular calculations.

Element	Functions	Ref.
H	5s2p1d	50
F	10s5p2d1f	50
Cl	15s9p2d1f	51
Br	24s17p11d1f	52 and 53
I	29s22p16d1f	52 and 53
Hg	30s24p15d11f1g	53 and 54
At	31s27p18d12f	52 and 53
Uus	31s30p21d13f	53 and 55

TABLE II. Spinor splittings (in hartree) for H-like ions with point charge nuclei.

SO Splitting	2cNESC	|2cNESC -4cDirac|	2cNESC	|2cNESC -4cDirac|
	Z = 120 (Ubn)		Z = 118 (Uuo)	
$2p_{3/2} - 2p_{1/2}$	708.2299530	$<10^{-8}$	637.1702111	$<10^{-8}$
$3p_{3/2} - 3p_{1/2}$	210.3266297	$<10^{-8}$	189.4477837	$<10^{-8}$
$4p_{3/2} - 4p_{1/2}$	86.0450533	$<10^{-8}$	77.6695049	$<10^{-8}$
$5p_{3/2} - 5p_{1/2}$	42.9111586	$<10^{-8}$	38.8334672	$<10^{-8}$
$6p_{3/2} - 6p_{1/2}$	24.6161441	$<10^{-8}$	22.4492488	$<10^{-8}$
$7p_{3/2} - 7p_{1/2}$	15.5620277	$<10^{-8}$	14.7098735	$<10^{-8}$
$3d_{5/2} - 3d_{3/2}$	39.3198991	$<10^{-8}$	36.5777309	$<10^{-8}$
$4d_{5/2} - 4d_{3/2}$	16.8647478	$<10^{-8}$	15.6801476	$<10^{-8}$
$5d_{5/2} - 5d_{3/2}$	8.6506004	$<10^{-8}$	8.0481371	$<10^{-8}$
$6d_{5/2} - 6d_{3/2}$	4.9897741	$<10^{-8}$	4.6707595	$<10^{-8}$
$4f_{7/2} - 4f_{5/2}$	7.5402554	$<10^{-8}$	7.0463923	$<10^{-8}$
$5f_{7/2} - 5f_{5/2}$	3.8568158	$<10^{-8}$	3.6068049	$<10^{-8}$
	Z = 112 (Cn)		Z = 102 (No)	
$2p_{3/2} - 2p_{1/2}$	467.2952021	$<10^{-8}$	281.1810867	$<10^{-8}$
$3p_{3/2} - 3p_{1/2}$	139.2516691	$<10^{-8}$	83.8991042	$<10^{-8}$
$4p_{3/2} - 4p_{1/2}$	57.3994720	$<10^{-8}$	34.7968676	$<10^{-8}$
$5p_{3/2} - 5p_{1/2}$	28.8569679	$<10^{-8}$	17.5014191	$<10^{-8}$
$6p_{3/2} - 6p_{1/2}$	16.8355283	$<10^{-8}$	9.8622180	$<10^{-8}$
$3d_{5/2} - 3d_{3/2}$	29.2580490	$<10^{-8}$	19.6858258	$<10^{-8}$
$4d_{5/2} - 4d_{3/2}$	12.5234974	$<10^{-8}$	8.4060985	$<10^{-8}$
$5d_{5/2} - 5d_{3/2}$	6.4397317	$<10^{-8}$	4.3179656	$<10^{-8}$
$6d_{5/2} - 6d_{3/2}$	3.8007357	$<10^{-8}$		
$4f_{7/2} - 4f_{5/2}$	5.7067868	$<10^{-8}$	3.9063215	$<10^{-8}$
$5f_{7/2} - 5f_{5/2}$	2.9269327	$<10^{-8}$	2.0086972	$<10^{-8}$

1.914 (HgF_2), 2.258 ($HgCl_2$), 2.381 ($HgBr_2$), and 2.568 Å (HgI_2).[59]

All calculations were carried out with a finite nucleus model possessing a Gaussian charge distribution.[13,60] Furthermore, a velocity of light $c = 137.035999070(98)$[61] was used throughout the article.

IV. RESULTS AND DISCUSSION

The 2cNESC/GHF method was tested for one-electron atoms by comparing their energies with 4cDirac/HF results (see Table II). For all test calculations (only some of which are given in Table II), deviations are 10^{-8} hartree or smaller thus verifying that 2cNESC is a Dirac-exact method.

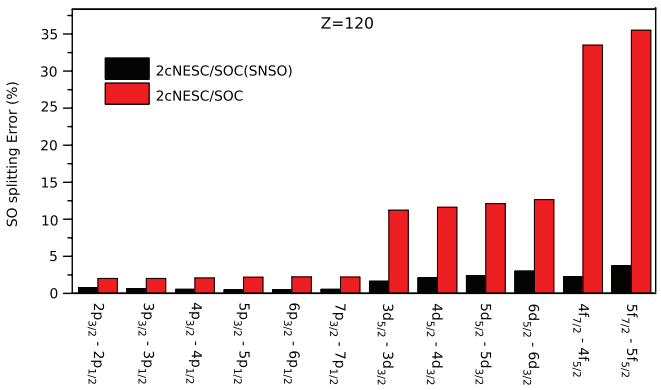

FIG. 1. Deviations (in percentage) of the 2cNESC(SNSO)/GHF spinor energy splittings from exact 4cDirac/HF splittings given in the case $Z = 120$.

Calculated 2cNESC(SNSO) spinor energy splittings of a series of elements are summarized in Table III and for molecules in Table IV. An analysis of the 2cNESC(SNSO) splittings for $Z = 120$ is provided in Figure 1. 2cNESC(SNSO) results for $HgX_2(^1\Sigma_g^+)$ molecules are analyzed in Table V and Figure 2, where the variation in the

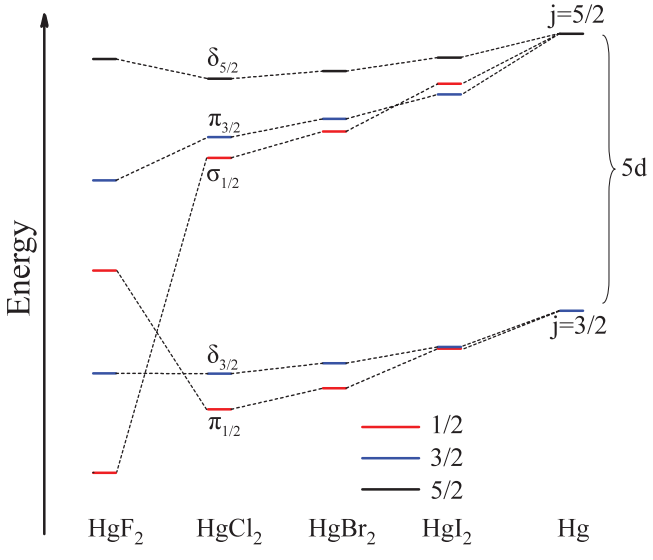

FIG. 2. Spinor diagram of $HgX_2(^1\Sigma_g^+)$ (X = F, Cl, Br, I) according to 2cNESC(SNSO)/GHF/cc-pVTZ calculations. Only the atomic $5d_{3/2}$ and $5d_{5/2}$ spinors and their ω counterparts for the HgX_2 molecule are shown.

TABLE III. SO splittings (in hartree) of neutral atoms by 4cDirac/HF, 2cNESC(SNSO)/GHF, and 2cNESC(mSNSO)/GHF with finite nucleus model. For atoms with Z > 109, mass number = 2.556*Z* is used. Relative deviations (in %) from the 4cDirac/HF values are given in parentheses.

SO splitting	4cDirac	2cNESC(SNSO)	2cNESC(mSNSO)	4cDirac	2cNESC(SNSO)	2cNESC(mSNSO)
		Z = 120 (Ubn)			Z = 118 (Uuo)	
$2p_{3/2} - 2p_{1/2}$	602.97483	598.35781(−0.8)	599.91195(−0.5)	543.15790	539.40129(−0.7)	540.40481(−0.5)
$3p_{3/2} - 3p_{1/2}$	148.45720	147.48688(−0.7)	148.04828(−0.3)	133.39014	132.61457(−0.6)	133.00921(−0.3)
$4p_{3/2} - 4p_{1/2}$	43.62587	43.38598(−0.5)	43.56142(−0.1)	38.99718	38.81046(−0.5)	38.93476(−0.2)
$5p_{3/2} - 5p_{1/2}$	13.05427	12.99054(−0.5)	13.04410(−0.1)	11.52191	11.47393(−0.4)	11.51147(−0.1)
$6p_{3/2} - 6p_{1/2}$	3.36826	3.35165(−0.5)	3.36646(−0.1)	2.86073	2.84876(−0.4)	2.85882(−0.1)
$7p_{3/2} - 7p_{1/2}$	0.61261	0.60923(−0.6)	0.61235(0.0)	0.43383	0.43164(−0.5)	0.43351(−0.1)
$3d_{5/2} - 3d_{3/2}$	22.65558	23.02624(1.6)	22.80864(0.7)	20.96930	21.30386(1.6)	21.09940(0.6)
$4d_{5/2} - 4d_{3/2}$	6.44391	6.57909(2.1)	6.51685(1.1)	5.91399	6.03671(2.1)	5.97875(1.1)
$5d_{5/2} - 5d_{3/2}$	1.76703	1.80947(2.4)	1.79220(1.4)	1.59221	1.63035(2.4)	1.61456(1.4)
$6d_{5/2} - 6d_{3/2}$	0.32862	0.33842(3.0)	0.33500(1.9)	0.27096	0.27922(3.0)	0.27634(2.0)
$4f_{7/2} - 4f_{5/2}$	1.90405	1.94659(2.2)	1.92853(1.3)	1.74004	1.77740(2.1)	1.76058(1.2)
$5f_{7/2} - 5f_{5/2}$	0.41754	0.43310(3.7)	0.42905(2.8)	0.36769	0.38151(3.8)	0.37787(2.8)
		Z = 112 (Cn)			Z = 102 (No)	
$2p_{3/2} - 2p_{1/2}$	398.63108	396.63663(−0.5)	396.67894(−0.5)	238.58099	237.97709(−0.3)	237.54685(−0.4)
$3p_{3/2} - 3p_{1/2}$	96.99132	96.61370(−0.4)	96.70685(−0.3)	56.91847	56.84539(−0.1)	56.77311(−0.3)
$4p_{3/2} - 4p_{1/2}$	27.86138	27.78141(−0.3)	27.81337(−0.2)	15.76109	15.75796(0.0)	15.73978(−0.1)
$5p_{3/2} - 5p_{1/2}$	7.89105	7.87363(−0.2)	7.88295(−0.1)	4.10567	4.10807(0.1)	4.10322(−0.1)
$6p_{3/2} - 6p_{1/2}$	1.70756	1.70398(−0.2)	1.70625(−0.1)	0.67831	0.67850(0.0)	0.67785(−0.1)
$3d_{5/2} - 3d_{3/2}$	16.48462	16.72960(1.5)	16.56080(0.5)	10.68904	10.83206(1.3)	10.71186(0.2)
$4d_{5/2} - 4d_{3/2}$	4.52386	4.61540(2.0)	4.56884(1.0)	2.77987	2.83500(2.0)	2.80357(0.9)
$5d_{5/2} - 5d_{3/2}$	1.14552	1.17300(2.4)	1.16107(1.4)	0.62446	0.63991(2.5)	0.63277(1.3)
$6d_{5/2} - 6d_{3/2}$	0.12064	0.11698(−3.0)	0.12376(2.6)			
$4f_{7/2} - 4f_{5/2}$	1.30923	1.33418(1.9)	1.32072(0.9)	0.77202	0.78421(1.6)	0.77526(0.4)
$5f_{7/2} - 5f_{5/2}$	0.24131	0.25092(4.0)	0.24836(2.9)	0.09731	0.10216(5.0)	0.10099(3.8)
		Z = 86 (Rn)			Z = 80 (Hg)	
$2p_{3/2} - 2p_{1/2}$	101.22751	101.27248(0.0)	100.90485(−0.3)	71.69802	71.79846(0.1)	71.49993(−0.3)
$3p_{3/2} - 3p_{1/2}$	23.16398	23.21241(0.2)	23.13400(−0.1)	16.09378	16.14595(0.3)	16.08193(−0.1)
$4p_{3/2} - 4p_{1/2}$	5.89896	5.91891(0.3)	5.89912(0.0)	3.93551	3.95371(0.5)	3.93805(0.1)
$5p_{3/2} - 5p_{1/2}$	1.23312	1.23896(0.5)	1.23472(0.1)	0.69595	0.70046(0.6)	0.69757(0.2)
$6p_{3/2} - 6p_{1/2}$	0.15636	0.15719(0.5)	0.15669(0.2)			
$3d_{5/2} - 3d_{3/2}$	4.80788	4.86365(1.2)	4.79884(−0.2)	3.41664	3.45377(1.1)	3.40392(−0.4)
$4d_{5/2} - 4d_{3/2}$	1.10938	1.13176(2.0)	1.11671(0.7)	0.74416	0.75933(2.0)	0.74839(0.6)
$5d_{5/2} - 5d_{3/2}$	0.17311	0.17823(3.0)	0.17583(1.6)	0.07542	0.07822(3.7)	0.07701(2.1)
$4f_{7/2} - 4f_{5/2}$	0.26558	0.26943(1.5)	0.26552(0.0)	0.16116	0.16382(1.7)	0.16117(0.0)
		Z = 54 (Xe)			Z = 48 (Cd)	
$2p_{3/2} - 2p_{1/2}$	11.97520	12.04279(0.6)	11.96205(−0.1)	7.10727	7.15478(0.7)	7.10055(−0.1)
$3p_{3/2} - 3p_{1/2}$	2.33470	2.35579(0.9)	2.34022(0.2)	1.30908	1.32300(1.1)	1.31309(0.3)
$4p_{3/2} - 4p_{1/2}$	0.46971	0.47468(1.1)	0.47148(0.4)	0.22465	0.22752(1.3)	0.22574(0.5)
$5p_{3/2} - 5p_{1/2}$	0.05277	0.05345(1.3)	0.05310(0.6)			
$3d_{5/2} - 3d_{3/2}$	0.48627	0.49156(1.1)	0.48036(−1.2)	0.26269	0.26536(1.0)	0.25838(−1.6)
$4d_{5/2} - 4d_{3/2}$	0.07757	0.07932(2.3)	0.07752(−0.1)	0.02935	0.03024(3.0)	0.02942(0.2)

spinor energies of molecules $HgX_2(^1\Sigma_g^+)$ for X = F, Cl, Br, I is displayed.

In Figure 1, the calculated 2cNESC(SNSO)/GHF spinor energy splittings for $Z = 120$ are compared with the corresponding exact Dirac/HF values by giving the deviations from the latter in percentage. The one-electron SO contributions (given in red) exaggerate calculated *np*-splittings on the average by 2%, *nd*-splittings by 10%, and *nf*-splittings by 33% where deviations become somewhat larger with increasing principal quantum number *n*. This exaggeration is largely corrected by the screened nucleus two-electron contributions so that final 2cNESC(SNSO) values differ by just 2% from the Dirac values. After the SNSO correction, deviations are 1% for *np*-splittings and increase to 3% for the *nf*-splittings where again deviations are somewhat larger for larger *n*.

The trends observed for $Z = 120$ are also valid for other elements. In Table III, the results obtained for noble gas elements xenon (Xe, $Z = 54$), radon (Rn, $Z = 86$), ununoctium (Uuo, $Z = 118$); group IIb elements cadmium (Cd, $Z = 48$), mercury (Hg, $Z = 80$), copernicium (Cn, $Z = 112$); the actinide nobelium (No, $Z = 102$), and finally unbinilium (Ubn, $Z = 120$) are listed, which are representative closed shell systems of periods 5, 6, 7, and 8. Deviations are largest (up to 4 hartree) when *Z* is large and core spinor energies with $n = 2$ are considered, which possess splittings up to 603 hartree ($Z = 120$ and $2p_{3/2} - 2p_{1/2}$). For valence spinors, deviations

TABLE IV. SO splittings (in cm^{-1}) of the valence np_π orbitals of HX and $5d_{\pi,\delta}$ orbitals of HgX_2 by 4cDirac/HF, 2cNESC(SNSO)/GHF and 2cNESC(mSNSO)/GHF with finite nucleus model (for Uus (Z = 117), a mass number of 2.556*Z* is used). Relative deviations (in %) from the 4cDirac/HF values are given in parentheses.

Mol.	Splitting	Dirac	2cNESC(SNSO)	2cNESC(mSNSO)
HF	$2p\pi_{3/2} - 2p\pi_{1/2}$	381	389(2.1)	371(−2.6)
HCl	$3p\pi_{3/2} - 3p\pi_{1/2}$	758	779(2.8)	762(0.5)
HBr	$4p\pi_{3/2} - 4p\pi_{1/2}$	2994	3056(2.1)	3025(1.0)
HI	$5p\pi_{3/2} - 5p\pi_{1/2}$	5942	6016(1.2)	5979(0.6)
HAt	$6p\pi_{3/2} - 6p\pi_{1/2}$	15 513	15 574(0.4)	15 538(0.2)
HUus	$7p\pi_{3/2} - 7p\pi_{1/2}$	23 955	23 968(0.1)	23 978(0.1)
HgF_2	$5d\pi_{3/2} - 5d\pi_{1/2}$	5362	5362(−0.4)	5357(−0.5)
	$5d\delta_{5/2} - 5d\delta_{3/2}$	18 769	19 316(2.9)	19 076(1.6)
$HgCl_2$	$5d\pi_{3/2} - 5d\pi_{1/2}$	16 266	16 821(3.4)	16 579(1.9)
	$5d\delta_{5/2} - 5d\delta_{3/2}$	17 613	18 214(3.4)	17 955(1.9)
$HgBr_2$	$5d\pi_{3/2} - 5d\pi_{1/2}$	16 095	16 660(3.5)	16 415(2.0)
	$5d\delta_{5/2} - 5d\delta_{3/2}$	17 446	18 056(3.5)	17 794(2.0)
HgI_2	$5d\pi_{3/2} - 5d\pi_{1/2}$	15 196	15 750(3.6)	15 506(2.0)
	$5d\delta_{5/2} - 5d\delta_{3/2}$	17 286	17 900(3.6)	17 637(2.0)

are just a few millihartrees. Since in these cases the splittings are just 1/3 to 2/3 of a hartree the relative deviations (given in %) appear to be large. For none of the elements considered, the relative deviation of the 2cNESC(SNSO) splittings exceeds 5% and, on average, the deviations are smaller than 2%. We note that, for each element investigated, a linear relationship between the 2cNESC(SNSO) and 4cDirac values can be established, which can help to reproduce the exact SO splittings from NESC data.

The observations made for the 2cNESC(SNSO) results in the case of the atoms are in line with those for the molecules although the SO splittings become somewhat smaller as a result of spinor-spinor interactions. In Table IV, calculated SO splittings in cm^{-1} are given for hydrogen halides HX (valence shell $np\pi$ splittings) with X = F, Cl, Br, I, At, Uus (ununseptium, $Z = 117$) and mercury(II) halides HgX_2 (mercury $5d\pi$ and $5d\delta$ splittings) with X = F, Cl, Br, I. For HX molecules, the splittings range from 381 to 23 955 cm^{-1} with the 2cNESC(SNSO)/GHF values always being somewhat larger (up to 60 cm^{-1}) indicating that the NESC values slightly exaggerate the splittings because of the approximate two-electron contributions to the SOC. However, the deviations when given in percentage are similar to those found for the atoms.

In the case of molecules HgX_2, absolute $5d\delta_{5/2} - 5d\delta_{3/2}$ and $5d\pi_{3/2} - 5d\pi_{1/2}$ splittings obtained with 2cNESC (SNSO)/GHF are also too large where deviations can increase to 600 cm^{-1}, which is still below 4% of the Dirac splittings for the heaviest homologues in the series (see Table IV). The use of the mSNSO parametrization reduces the relative deviations by approximately a factor of two. Generally, the overall magnitude and the relative precision of the calculated SO splittings for the HgX_2 molecules is of the same order of magnitude as for the bare Hg atom. This is to be expected as the $5d\delta_{5/2}$ and $5d\pi_{3/2}$ spinors can be traced back to the atomic $5d_{5/2}$ spinors and the $5d\delta_{3/2}$ and $5d\pi_{1/2}$ to the atomic $5d_{3/2}$ spinors (see Table 7.2 in Ref. 13). We note that here and in the following, we distinguish between different ω-spinors with the same symmetry by labeling them according to the dominant spin-free orbital.

The valence spinors of HgX_2 are analyzed in Table V by decomposing them in terms of the corresponding spin-free atomic orbitals of the Hg and X atoms. The spin-free atomic orbitals are labeled by the projection of the orbital angular momentum on the molecular axis (σ-, π-, or δ-type). As follows from Table V, the spinor with the highest projection of the total angular momentum on the molecular axis, $\omega = 5/2$, is a pure δ-type 5d atomic orbital of Hg as it does not mix

TABLE V. Spinor population analysis for the HgX_2 molecules based on the results of 2cNESC(SNSO) calculations.

Mol.	Spinor	Energy (a.u.)	Contribution (%)
HgF2	1/2	−0.78610	$Hg5d_\sigma$ (36) + $Hg5d_\pi$ (39) + $F2s_\sigma$ (2) + $F2p_\sigma$ (18) + $F2p_\pi$ (5)
	1/2	−0.72898	$Hg5d_\sigma$ (20) + $Hg5d_\pi$ (43) + $F2s_\sigma$ (1) + $F2p_\sigma$ (23) + $F2p_\pi$ (12)
	3/2	−0.75917	$Hg5d_\pi$ (38) + $Hg5d_\delta$ (55) + $F2p_\pi$ (7)
	3/2	−0.70455	$Hg5d_\pi$ (39) + $Hg5d_\delta$ (44) + $F2p_\pi$ (17)
	5/2	−0.67116	$Hg5d_\delta$ (100)
HgCl2	1/2	−0.76920	$Hg5d_\sigma$ (30) + $Hg5d_\pi$ (60) + $Cl3s_\sigma$ (3) + $Cl3p_\sigma$ (4) + $Cl3p_\pi$ (2)
	1/2	−0.69823	$Hg5d_\sigma$ (45) + $Hg5d_\pi$ (35) + $Cl3s_\sigma$ (4) + $Cl3p_\sigma$ (13) + $Cl3p_\pi$ (2)
	3/2	−0.75963	$Hg5d_\pi$ (29) + $Hg5d_\delta$ (70) + $Cl3p_\pi$ (1)
	3/2	−0.69256	$Hg5d_\pi$ (66) + $Hg5d_\delta$ (30) + $Cl3p_\pi$ (4)
	5/2	−0.67664	$Hg5d_\delta$ (100)
HgBr2	1/2	−0.76350	$Hg5d_\sigma$ (30) + $Hg5d_\pi$ (62) + $Br4s_\sigma$ (3) + $Br4p_\sigma$ (3) + $Br4p_\pi$ (1)
	1/2	−0.69109	$Hg5d_\sigma$ (49) + $Hg5d_\pi$ (34) + $Br4s_\sigma$ (4) + $Br4p_\sigma$ (10) + $Br4p_\pi$ (2)
	3/2	−0.75683	$Hg5d_\pi$ (27) + $Hg5d_\delta$ (72) + $Br4p_\pi$ (1)
	3/2	−0.68759	$Hg5d_\pi$ (69) + $Hg5d_\delta$ (28) + $Br4p_\pi$ (3)
	5/2	−0.67456	$Hg5d_\delta$ (100)
HgI2	1/2	−0.75269	$Hg5d_\sigma$ (24) + $Hg5d_\pi$ (68) + $I5s_\sigma$ (6) + $I5p_\sigma$ (1) + $I5p_\pi$ (1)
	1/2	−0.67813	$Hg5d_\sigma$ (55) + $Hg5d_\pi$ (29) + $I5s_\sigma$ (8) + $I5p_\sigma$ (6) + $I5p_\pi$ (1)
	3/2	−0.75242	$Hg5d_\pi$ (25) + $Hg5d_\delta$ (74)
	3/2	−0.68093	$Hg5d_\pi$ (72) + $Hg5d_\delta$ (26) + $I5p_\pi$ (1)
	5/2	−0.67086	$Hg5d_\delta$ (100)

with any other spin-free orbitals. Consequently, the energy of the $5d\delta_{5/2}$ spinor remains nearly constant within the HgX_2 series. The $\omega = 3/2$ spinors in HgX_2 comprise δ and π spin-free atomic orbitals, with the former making a dominating contribution to the lower energy spinor (henceforth labeled $5d\delta_{3/2}$) and the latter dominating the higher energy spinor ($5d\pi_{3/2}$). Mixing of the spin-free orbitals in the $\omega = 3/2$ spinors results in a lowering of the energy of the $5d\delta_{3/2}$ spinor and a rising of the energy of the $5d\pi_{3/2}$ one. The $\omega = 1/2$ spinors comprise π and σ spin-free atomic orbitals of Hg and X; however, their relative contribution to the higher and the lower energy spinor vary along the series X = F, Cl, Br, I. For X = Cl, Br, and I, the lower energy $\omega = 1/2$ spinor is dominated by the π-type spin-free atomic orbitals and the higher energy spinor by the σ-type orbitals. For X = F, the increased participation of the ligand orbitals in the chemical bond results in an inversion of the ordering of the $\omega = 1/2$ spinors so that $5d\sigma_{1/2}$ becomes the lowest energy molecular spinor.

Figure 2 shows the energies of the valence spinors of molecules HgX_2, which are classified according to the analysis given above. It is apparent from the diagram that the splitting of the molecular spinors corresponds to the strong SOC limit being perturbed by the interactions with the ligands. The influence of the ligand field increases from I to F thus leading to a greater scatter of the molecular spinors and, for HgF_2, even resulting in a change of the character of the lowest energy spinor (from π to σ) shown in Figure 2. Hence, the $5d\pi_{3/2} - 5d\pi_{1/2}$ energy difference in Table IV abruptly decreases in magnitude for HgF_2 as compared to the heavier HgX_2 homologues. From the $5d\pi_{3/2} - 5d\pi_{1/2}$ and $5d\delta_{5/2} - 5d\delta_{3/2}$ spinor splittings in Table IV, it can be concluded that 2cNESC(SNSO) and 2cNESC(mSNSO) are capable of describing the ligand field effect on the spinor energies with a sufficiently high accuracy. For instance, the $5d\delta_{5/2} - 5d\pi_{3/2}$ splittings calculated for HgX_2 with 2cNESC(SNSO) or 2cNESC(mSNSO) (not reported in Table IV) deviate from the reference 4cDirac/HF values by just 0.5 – 0.1 %.

The effect of SOC on the atomization energies of molecules HX and HgX_2 is illustrated by the data in Table VI where total and atomization energies obtained with the 2cNESC(mSNSO)/GHF method are compared with the corresponding spin-free NESC/UHF results. The atomization energy of molecules HX is reduced due to quenching of the atomic SOC effect upon H–X bond formation. The magnitude of the reduction varies between 0.46 kcal/mol for F and 19.31 kcal/mol for Uus, thus underlining the importance of the SOC effect for bonding when involving heavy elements. Compared to HX, the presence of a heavy central atom in HgX_2 slightly stabilizes the bonding as can be judged from the analysis of the overall SOC effect on the atomization energy. The latter can be determined from the difference $\Delta\Delta E_{at}^{SO} = \Delta E_{at}^{SO} - \Delta E_{at}^{SF}$ (calculated for HgX_2) by subtracting the SOC of HX, i.e., $\Delta\Delta E_{at}^{SO}(HgX_2) - 2 * \Delta\Delta E_{at}^{SO}(HX)$. Although this stabilization is weak and varies just from 0.85 kcal/mol for HgF_2 to 1.51 kcal/mol for HgI_2, it may nevertheless lead to a slight SOC-caused shortening of the equilibrium bond length. According to 2cNESC(mSNSO)/PBE0 calculations, which will be published in more detail elsewhere, SOC causes a shortening of the Hg–F bond in HgF_2 from 1.915 to 1.912 Å.

TABLE VI. Total energy E (in a.u.) and atomization energy ΔE_{at} (in kcal/mol) of molecules HX and HgX_2 (X = F, Cl, Br, I, At, and Uus) obtained at the 2cNESC(mSNSO)/GHF (SO) and the spin-free NESC/UHF (SF) levels of theory. The total energy of the H atom is −0.4998163 a.u. and those of the Hg atom are −19639.8986633 a.u. (SO) and −19620.1625575 a.u. (SF). For the geometries used, see text.

Mol.		E(molecule) (a.u.)	E(X) (a.u.)	ΔE_{at} (kcal/mol)
HF	SO	− 100.1442402	− 99.4931781	94.91
	SF	− 100.1442363	− 99.4924413	95.37
HCl	SO	− 461.5198133	− 460.9018977	74.11
	SF	− 461.5193975	− 460.8984868	75.99
HBr	SO	− 2605.1717492	− 2604.5757704	60.34
	SF	− 2605.1046016	− 2604.5025381	64.16
HI	SO	− 7114.4638098	− 7113.8926542	44.77
	SF	− 7113.3400713	− 7112.7571824	52.13
HAt	SO	− 22 898.7973892	− 22898.2525965	28.22
	SF	− 22 868.0286211	− 22867.4577339	44.60
HUus	SO	− 53 440.0056758	− 53439.4820413	14.95
	SF	− 53 031.7314499	− 53031.1770363	34.26
HgF_2	SO	− 19 838.9791412	− 99.4931781	59.06
	SF	− 19 819.2416782	− 99.4924413	59.13
$HgCl_2$	SO	− 20 561.8138405	− 460.9018977	69.89
	SF	− 20 542.0753633	− 460.8984868	72.68
$HgBr_2$	SO	− 24 849.1398133	− 2604.5757704	56.23
	SF	− 24 829.2676121	− 2604.5025381	62.74
HgI_2	SO	− 33 867.7432420	− 7113.8926542	37.19
	SF	− 33 845.7572404	− 7112.7571824	50.40

The observed strengthening of the Hg–X bonds can be explained by a lowering of the ground state energy of HgX_2 due to the second-order SOC contribution. The effect of the second-order SOC increases with increasing nuclear charge Z of ligand X due to (a) an overall increase of the magnitude of the SOC effect for larger Z and (b) a decrease of the electronegativity of X, which results in a greater electron population of the Hg valence orbitals (spinors).

V. CONCLUSIONS

In this work, we have extended the NESC algorithm developed previously[4] to a two-component approach that can be used for the calculation of the SOC effect. The new approach, abbreviated as 2cNESC(SNSO) (or 2cNESC(mSNSO), if adjusted SNSO parameters are used), is based on an effective one-electron SOC operator that employs the screened-nucleus potential of Boettger[30] in an improved version for higher angular momentum quantum numbers and with slightly adjusted parameters, which makes it possible to obtain reliable SO splittings for atoms and molecules with Z values up to 120 with an accuracy that almost matches exact 4cDirac calculations as reflected by an average deviation of less than 2%. 2cNESC(mSNSO) can easily compete with AMFI and other two-component methods based on an effective one-electron SOC operator.

It is noteworthy that relativistic methods provide a deeper, more consistent insight into bonding patterns of molecules containing heavy atoms than can be achieved with the use of spin-free relativistic or non-relativistic methods.

This is demonstrated for the series of HgX_2, X = F, Cl, Br, I, molecules, for which the interplay between the SOC and ligand field effects leads to changing the character of low-lying valence spinor from predominantly σ-type to π-type.

ACKNOWLEDGMENTS

This work was financially supported by the National Science Foundation, Grant No. CHE 1152357. We thank SMU for providing computational resources. The authors are indebted to an unknown referee for fruitful comments, which led to improvement of the paper.

[1]K. G. Dyall, J. Chem. Phys. **106**, 9618 (1997).
[2]M. Filatov and K. G. Dyall, Theor. Chem. Acc. **117**, 333 (2007).
[3]P. A. M. Dirac, Proc. R. Soc. London, Ser. A **117**, 610 (1928).
[4]W. Zou, M. Filatov, and D. Cremer, Theor. Chem. Acc. **130**, 633 (2011).
[5]W. Zou, M. Filatov, and D. Cremer, J. Chem. Phys. **134**, 244117 (2011).
[6]W. Zou, M. Filatov, and D. Cremer, J. Chem. Phys. **137**, 084108 (2012).
[7]M. Filatov, W. Zou, and D. Cremer, J. Phys. Chem. A **116**, 3481 (2012).
[8]M. Filatov, W. Zou, and D. Cremer, J. Chem. Theor. Comput. **8**, 875 (2012).
[9]M. Filatov, W. Zou, and D. Cremer, J. Chem. Phys. **137**, 054113 (2012).
[10]W. Zou, M. Filatov, and D. Cremer, J. Chem. Theory Comput. **8**, 2617 (2012).
[11]W. Zou, M. Filatov, D. Atwood, and D. Cremer, Inorg. Chem. **52**, 2497 (2013).
[12]M. Filatov, W. Zou, and D. Cremer, J. Chem. Phys. **137**, 131102 (2012).
[13]K. G. Dyall and K. Fægri, *Introduction to Relativistic Quantum Chemistry* (Oxford University Press, Oxford, 2007).
[14]T. R. Furlani and H. F. King, J. Chem. Phys. **82**, 5577 (1985).
[15]D. G. Fedorov, S. Koseki, M. W. Schmidt, and M. S. Gordon, Int. Rev. Phys. Chem. **22**, 551 (2003).
[16]C. M. Marian, WIREs Comput. Mol. Sci. **2**, 187 (2012).
[17]W. Liu, Mol. Phys. **108**, 1679 (2010).
[18]T. Saue, ChemPhysChem **12**, 3077 (2011).
[19]D. Peng and M. Reiher, Theor. Chem. Acc. **131**, 1081 (2012).
[20]T. Fleig, Chem. Phys. **395**, 2 (2012).
[21]E. Kraka, W. Zou, M. Freindorf, and D. Cremer, J. Chem. Theory Comput. **8**, 4931 (2012).
[22]A. Berning, M. Schweizer, H.-J. Werner, P. J. Knowles, and P. Palmieri, Mol. Phys. **98**, 1823 (2000).
[23]S. Coriani, T. Helgaker, P. Jørgensen, and W. Klopper, J. Chem. Phys. **121**, 6591 (2004).
[24]D. G. Fedorov and M. S. Gordon, J. Chem. Phys. **112**, 5611 (2000).
[25]O. Vahtras, M. Engström, and B. Schimmelpfennig, Chem. Phys. Lett. **351**, 424 (2002).
[26]J. Tatchen, M. Kleinschmidt, and C. M. Marian, J. Chem. Phys. **130**, 154106 (2009).
[27]H. F. King and T. R. Furlani, J. Comput. Chem. **9**, 771 (1988).
[28]B. A. Hess, C. M. Marian, U. Wahlgren, and O. Gropen, Chem. Phys. Lett. **251**, 365 (1996).
[29]B. Schimmelpfennig, *AMFI: Atomic Mean Field Integral Program* (University of Stockholm, Stockholm, Sweden, 1996).
[30]J. C. Boettger, Phys. Rev. B **62**, 7809 (2000).
[31]M. Douglas and N. M. Kroll, Ann. Phys. (N.Y.) **82**, 89 (1974).
[32]B. A. Hess, Phys. Rev. A **32**, 756 (1985).
[33]B. A. Hess, Phys. Rev. A **33**, 3742 (1986).
[34]S. Majumder, A. V. Matveev, and N. Rösch, Chem. Phys. Lett. **382**, 186 (2003).
[35]J. E. Peralta and G. E. Scuseria, J. Chem. Phys. **120**, 5875 (2004).
[36]C. van Wüllen and C. Michauk, J. Chem. Phys. **123**, 204113 (2005).
[37]R. Seeger and J. A. Pople, J. Chem. Phys. **66**, 3045 (1977).
[38]S. Hammes-Schiffer and H. C. Andersen, J. Chem. Phys. **99**, 1901 (1993).
[39]M. Iliaš and T. Saue, J. Chem. Phys. **126**, 064102 (2007).
[40]K. G. Dyall, J. Comp. Chem. **23**, 786 (2002).
[41]W. Liu and D. Peng, J. Chem. Phys. **131**, 031104 (2009).
[42]Z. Li, Y. Xiao, and W. Liu, J. Chem. Phys. **137**, 154114 (2012).
[43]K. G. Dyall and E. van Lenthe, J. Chem. Phys. **111**, 1366 (1999).
[44]M. Filatov and D. Cremer, J. Chem. Phys. **119**, 1412 (2003).
[45]C. A. Jimez-Hoyos, T. M. Henderson, and G. E. Scuseria, J. Chem. Theory Comput. **7**, 2667 (2011).
[46]E. Kraka, M. Filatov, W. Zou, J. Gräfenstein, D. Izotov, J. Gauss, Y. He, A. Wu, V. Polo, L. Olsson, Z. Konkoli, Z. He, and D. Cremer, COLOGNE, a quantum chemical electronic structure program, Release COLOGNE12 (Southern Methodist University, Dallas, TX, 2012).
[47]A. Wolf, M. Reiher, and B. A. Hess, J. Chem. Phys. **117**, 9215 (2002).
[48]G. L. Malli, A. B. F. D. Silva, and Y. Ishikawa, J. Chem. Phys. **101**, 6829 (1994).
[49]H. J. Aa. Jensen, R. Bast, T. Saue, and L. Visscher, with contributions from V. Bakken, K. G. Dyall, S. Dubillard, U. Ekström, E. Eliav, T. Enevoldsen, T. Fleig, O. Fossgaard, A. S. P. Gomes, T. Helgaker, J. K. Lærdahl, Y. S. Lee, J. Henriksson, M. Iliaš, Ch. R. Jacob, S. Knecht, S. Komorovský, O. Kullie, C. V. Larsen, H. S. Nataraj, P. Norman, G. Olejniczak, J. Olsen, Y. C. Park, J. K. Pedersen, M. Pernpointner, K. Ruud, P. Sałek, B. Schimmelpfennig, J. Sikkema, A. J. Thorvaldsen, J. Thyssen, J. van Stralen, S. Villaume, O. Visser, T. Winther, and S. Yamamoto, DIRAC, a relativistic *ab initio* electronic structure program, Release DIRAC12, 2012, see http://www.diracprogram.org.
[50]T. H. Dunning, Jr., J. Chem. Phys. **90**, 1007 (1989).
[51]D. E. Woon and T. H. Dunning, Jr., J. Chem. Phys. **98**, 1358 (1993).
[52]K. G. Dyall, Theor. Chem. Acc. **115**, 441 (2006).
[53]See http://dirac.chem.sdu.dk/basisarchives/dyall/index.html for Dyall basis sets.
[54]A. S. P. Gomes and K. G. Dyall, Theor. Chem. Acc. **125**, 97 (2010).
[55]K. G. Dyall, Theor. Chem. Acc. **131**, 1172 (2012).
[56]G. Herzberg and K.-P. Huber, *Molecular Spectra and Molecular Structure* (Van Nostrand, New York, 1979), Vol. IV.
[57]F. Wang, J. Gauss, and C. van Wüllen, J. Chem. Phys. **129**, 064113 (2008).
[58]Y.-K. Han, C. Bae, S.-K. Son, and Y. S. Lee, J. Chem. Phys. **112**, 2684 (2000).
[59]J. Kim, H. Ihee, and Y. S. Lee, J. Chem. Phys. **133**, 144309 (2010).
[60]L. Visscher and K. G. Dyall, At. Data Nucl. Data Tables **67**, 207 (1997).
[61]G. Gabrielse, D. Hanneke, T. Kinoshita, M. Nio, and B. Odom, Phys. Rev. Lett. **97**, 030802 (2006).